Supplement of Atmos. Chem. Phys., 21, 5777–5806, 2021
https://doi.org/10.5194/acp-21-5777-2021-supplement
© Author(s) 2021. CC BY 4.0 License.

Atmospheric Chemistry and Physics
Open Access
EGU

Supplement of

Effects of prescribed CMIP6 ozone on simulating the Southern Hemisphere atmospheric circulation response to ozone depletion

Ioana Ivanciu et al.

Correspondence to: Ioana Ivanciu (iivanciu@geomar.de)

The copyright of individual parts of the supplement might differ from the article licence.

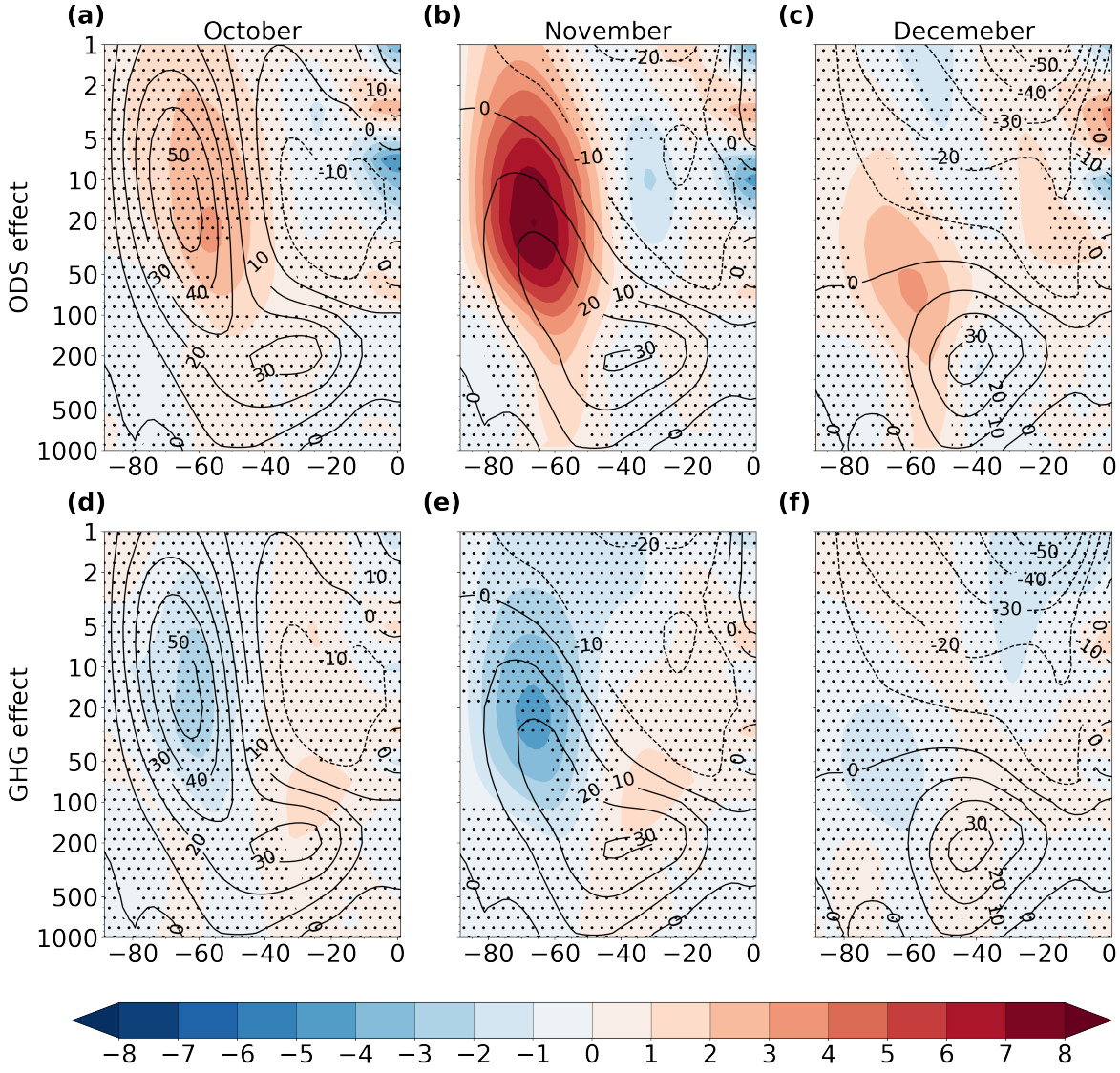

Figure S1. Latitude-height zonal wind difference between REF and NoODS (a, b and c) and between REF and NoGHG (d, e and f) for October (a and d), November (b and e) and December (c and f) in $\mathrm{m\ s^{-1}}$ (color shading). Stippling masks values that are not significant at the 95% confidence interval. The overlaying contours mark the 1978-2002 climatology of each respective month from REF.

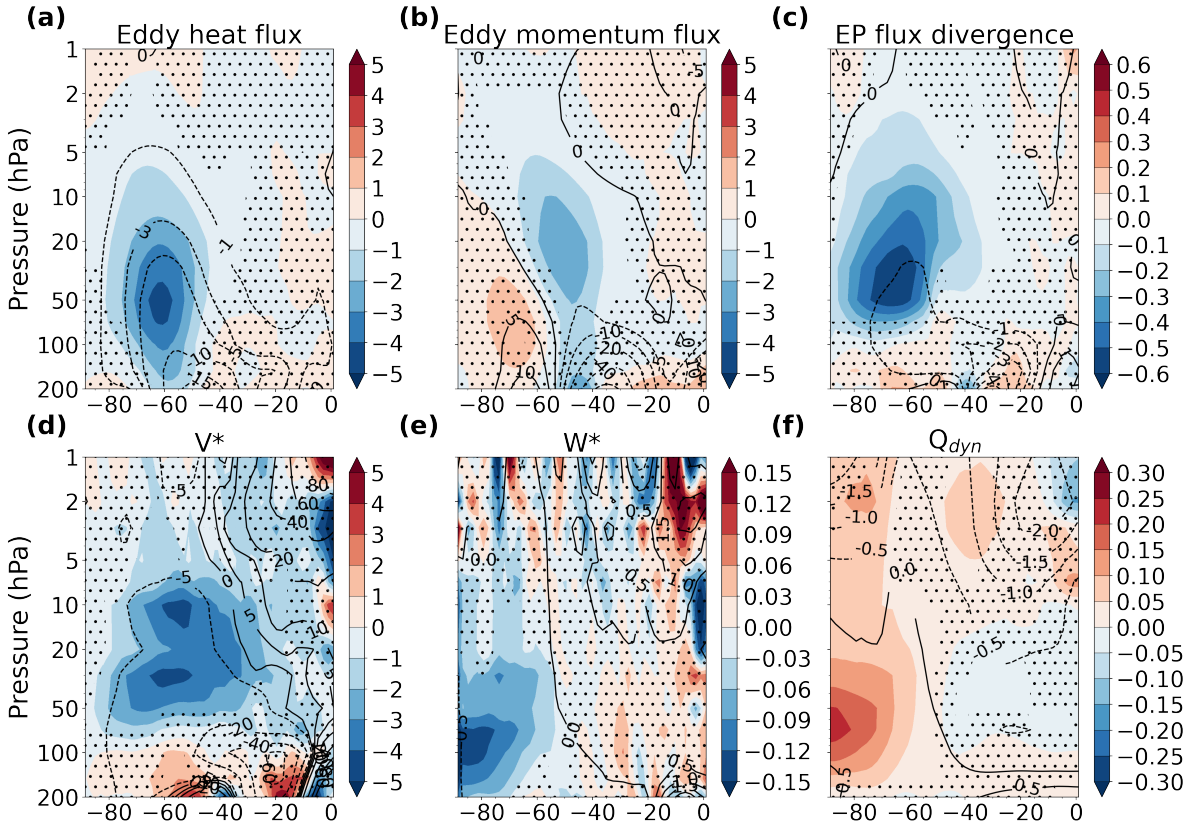

Figure S2. Latitude-height December difference between REF and NoODS in the eddy heat flux (a, in K $\mathrm{m\ s^{-1}}$), the eddy momentum flux (b, in $\mathrm{m^2 s^{-2}}$), the divergence of the EP flux (c, in $\mathrm{m\ s^{-1}\ day^{-1}}$), the meridional residual velocity (d, in $\mathrm{cm\ s^{-1}}$), the vertical residual velocity (e, in $\mathrm{mm\ s^{-1}}$) and in the dynamical heating rate (f, in K $\mathrm{day^{-1}}$) for the period 1978-2002 (color shading). Contours in each panel show the corresponding climatology from REF. Stippling masks values that are not significant at the 95% confidence interval.

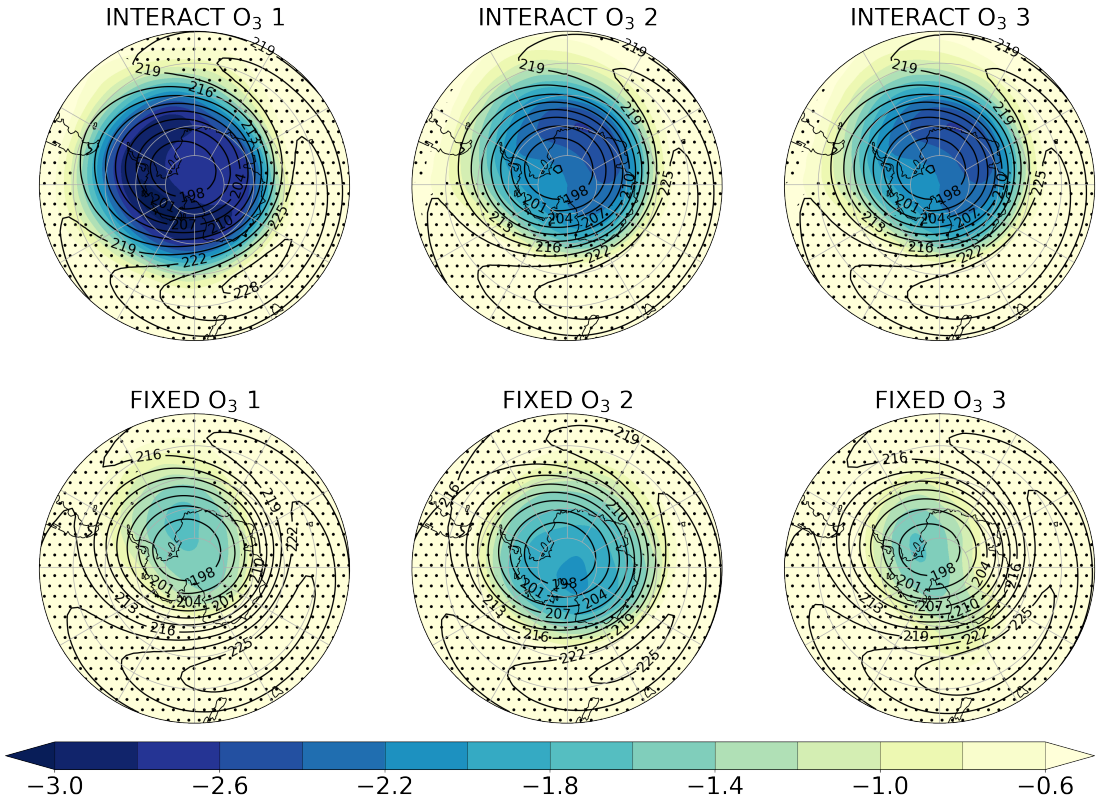

Figure S3. Polar stereographic maps of the October 70 hPa temperature trends for the individual members of INTERACT O_3 (a-c) and FIXED O_3 (d-f) in K dec^{-1} for the period 1958-2002 (color shading). The contours show the October climatological temperature in each simulations. Stippling masks regions where the trends are not significant at the 95% confidence level.

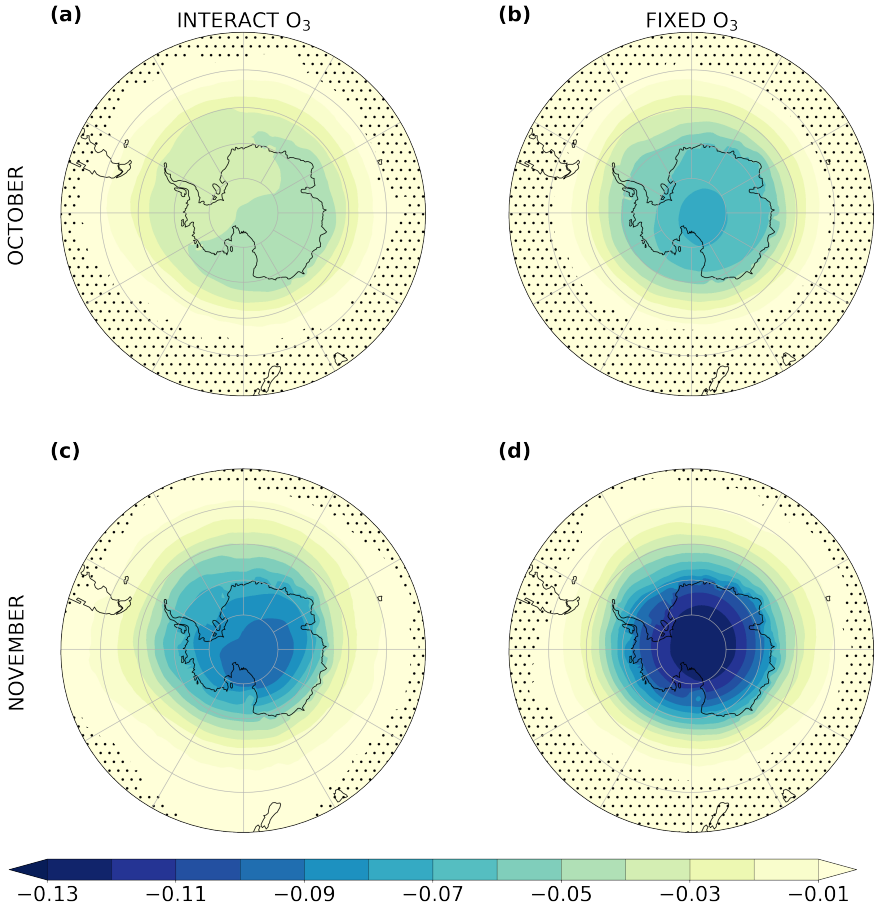

Figure S4. Polar stereographic maps of the October (a and b) and November (c and d) 100 hPa trends in SW heating rate for INTERACT O_3 (a and c) and FIXED O_3 (b and d) in K day^{-1} dec^{-1} for the period 1958-2002. Stippling masks regions where the trends are not significant at the 95% confidence level.

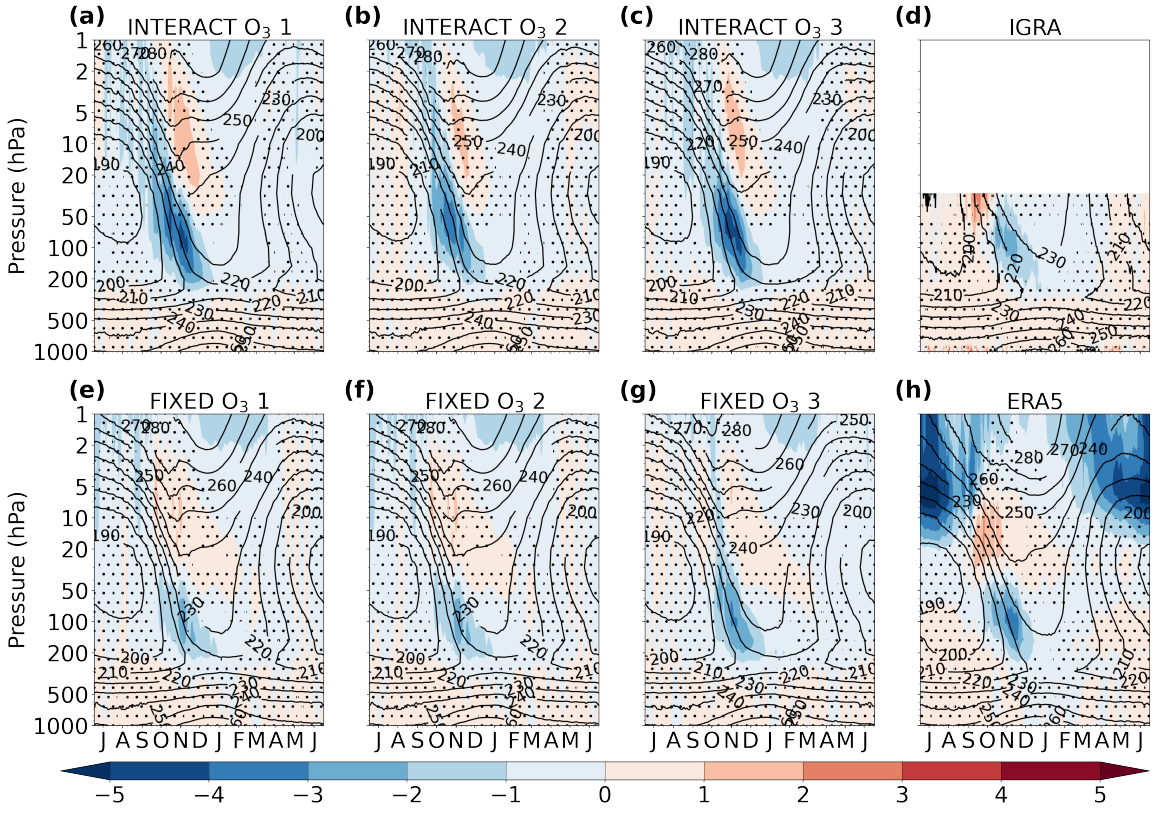

Figure S5. Seasonal cycle of the polar cap (65°S-90°S) temperature trend for the individual members of INTERACT O_3 (a-c) and FIXED O_3 (e-g) and for IGRA (d) and ERA5 (h) for the period 1958-2002 in K dec^{-1} (color shading). Stippling masks regions where the trends are not significant at the 95% confidence level. The overlaying contours show the corresponding climatological seasonal cycle. The letter corresponding to each month marks the middle of that month.

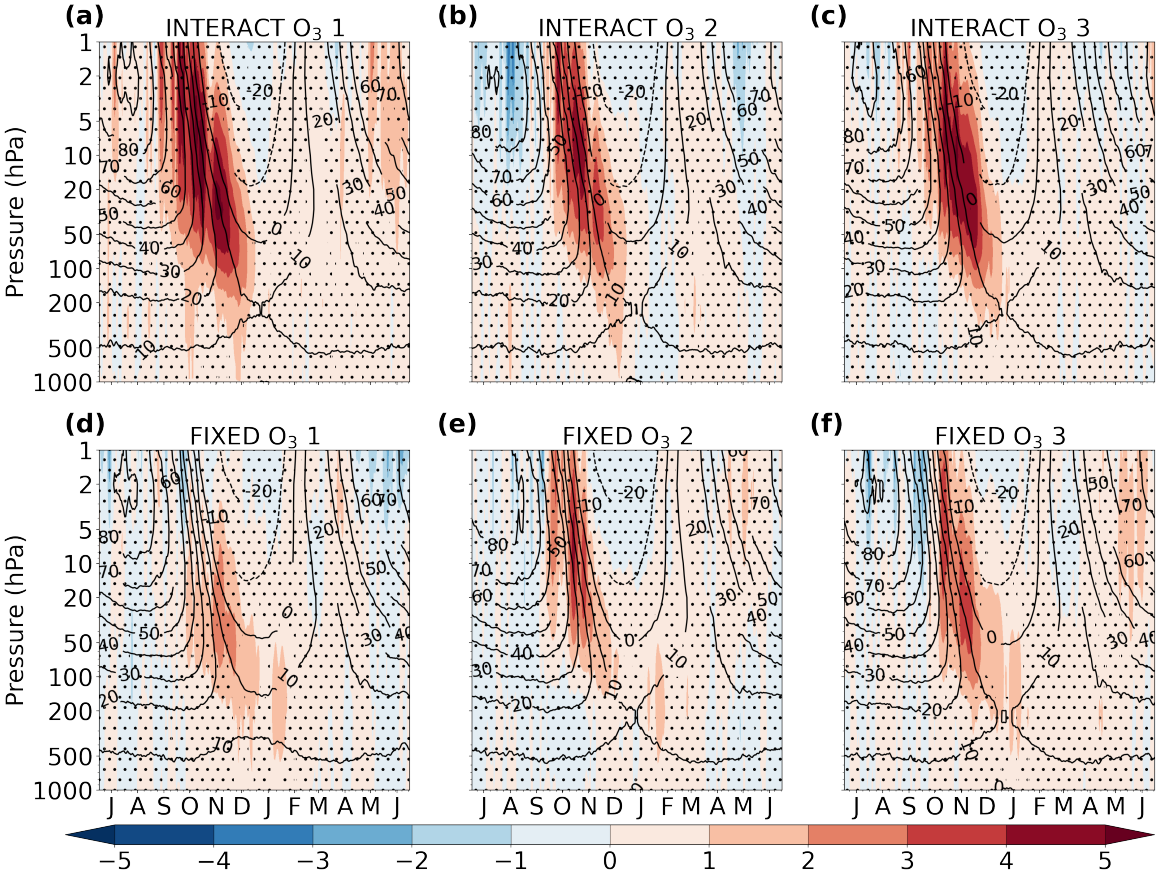

Figure S6. Seasonal cycle of the 50°S-70°S zonal wind trend for the individual members of INTERACT O_3 (a-c) and FIXED O_3 (d-f) for the period 1958-2002 in $\mathrm{m\ s^{-1}\ dec^{-1}}$ (color shading). Stippling masks regions where the trends are not significant at the 95% confidence level. The overlaying contours show the corresponding climatological seasonal cycle. The letter corresponding to each month marks the middle of that month.

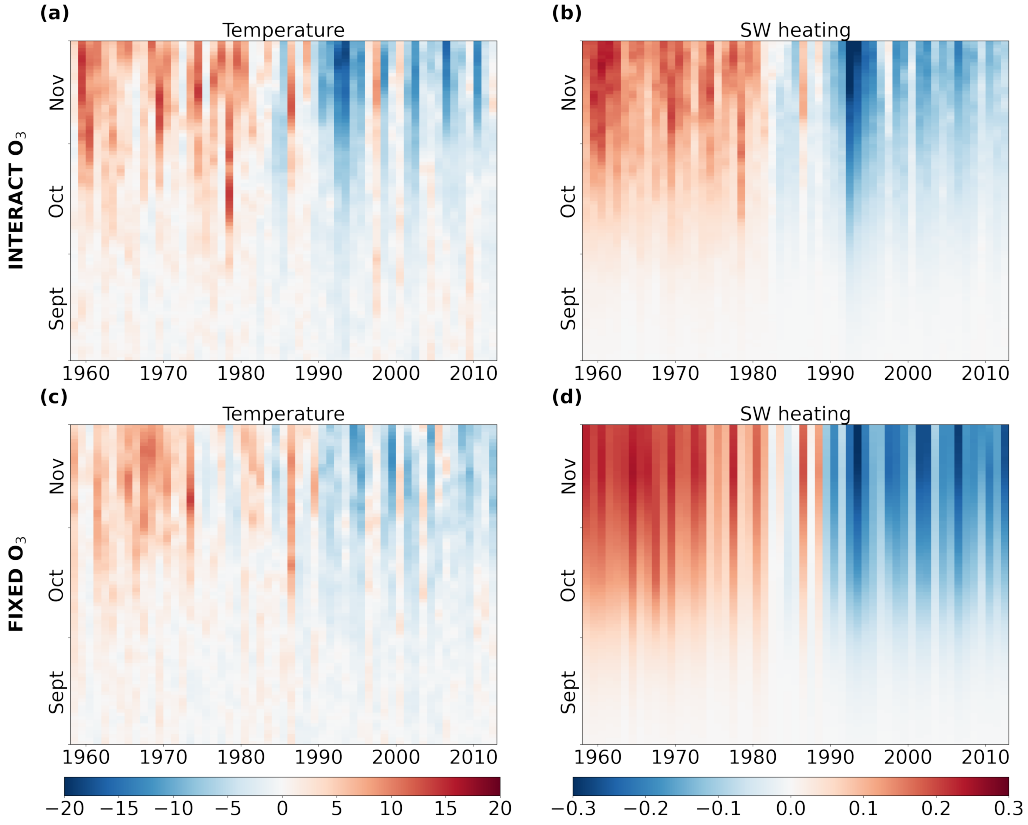

Figure S7. Timeseries of INTERACT O_3 (a, b) and FIXED O_3 (c, d) 100 hPa polar cap (70°S-90°S) temperature (a, c, in K) and SW heating rate (b, d, in $\mathrm{K\ day^{-1}}$) anomalies with respect to the 1958-2013 climatology for each austral spring day.

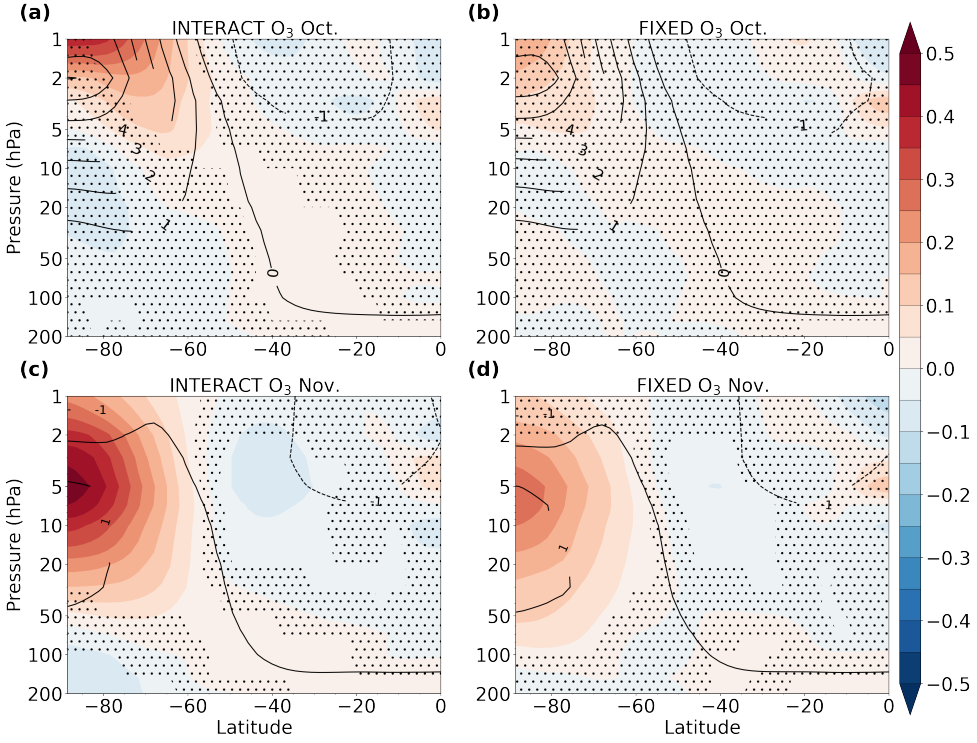

Figure S8. Latitude-height trends in October (a and b) and November (c and d) dynamical heating rate (in K day^{-1} dec^{-1}) in INTERACT O_3 (a and c) and FIXED O_3 (b and d) for the period 1958-2002 (color shading). Stippling masks the trends that are not significant at the 95% confidence interval. The overlaying contours in each panel show the corresponding climatologies.